

ARTICLE

Advances in Cytochemical Methods for Detection of Apoptosis

Katherine L. Barrett, Jonathan M. Willingham, A. Julian Garvin, and Mark C. Willingham

Department of Pathology, Wake Forest University School of Medicine, Winston–Salem, North Carolina

SUMMARY In an earlier article from this laboratory, the current methods developed to detect apoptosis in cells and tissues were highlighted, along with the challenges in their interpretation. Recent discoveries concerning the underlying biochemical mechanisms of apoptotic effector pathways have made possible further assays that allow a more direct measure of the activation of the apoptotic machinery in cells. This article summarizes some of these newer methods and extends the interpretation of the more classical assays of apoptosis in a defined cell system. We present data in KB and PC3 cell model culture systems induced to undergo apoptosis by the plant toxin ricin. Using a modified *in situ* nick translation assay (ISNT) with either Bodipy or BUdR labeling, we confirm that most cells showing altered nuclear morphology do not show reactivity with this assay until very late in the apoptotic process. We also show that only a minority of cells label with fluorescent annexin V during apoptosis but that apoptotic cells continue to internalize material from the cell surface through endocytosis after becoming reactive with annexin V. In addition, we describe the utility of a prototype of new assays for caspase substrate cleavage products, the detection of cleaved cytokeratin 18. It is these newer cleavage product assays that perhaps hold the greatest promise for specific detection of apoptosis in cells either in cell culture or in intact tissues. (J Histochem Cytochem 49:821–832, 2001)

KEY WORDS

apoptosis
cytochemistry
TUNEL
ISNT
annexin V
caspases
ricin

THE REGULATION of apoptosis has gained central importance in many aspects of biology, including studies of embryonic development, the pathogenesis of disease, and the response of cells to therapy (Wyllie 1992). The accurate detection of apoptosis has therefore become crucial to these studies. Beginning with the initial observations of changes in nuclear morphology that distinguished apoptosis from necrotic cell death, the field of cell death research has rapidly expanded, generating a wealth of knowledge about the genetic and biochemical pathways that control this process (reviewed in Green 2000). Several assays for detection of apoptosis were also developed during this past decade, some of which were applicable to cytochemical analysis. However, the interpretation and specificity of these assays, especially the TUNEL assay for DNA strand breaks, have been points of contro-

versy (Allen et al. 1997). These issues have been presented in a previous article from this laboratory, in which we reviewed the available methods for apoptosis detection (Willingham 1999). The present article builds on this prior review, presents some limited new data on modifications of older methods, and reviews some newer methods for apoptosis detection.

Figure 1 summarizes a small portion of the apoptosis regulation pathways that have been recently delineated, and it is clear that this new knowledge can be the starting point for the design of more specific assays of apoptosis. Several new assays have recently appeared that depend on newly discovered changes at the molecular level. These changes are relatively more specific for the apoptotic process and offer the possibility of removing some of the controversy surrounding older detection methods. In this article, we describe our recent studies evaluating *in situ* nick translation (ISNT) methods using Bodipy and BUdR labeling, annexin V binding, and the detection of a caspase-specific cleavage product (cytokeratin 18) in a model system of apoptosis utilizing ricin-induced apoptosis of KB and PC3 cells. This assay system is similar to our previously presented systems in which we

Correspondence to: Mark C. Willingham, Dept. of Pathology, Wake Forest Univ. School of Medicine, Gray Bldg., Room 2106, Medical Center Blvd., Winston–Salem, NC 27157. E-mail: mwilling@wfubmc.edu

Received for publication November 17, 2000; accepted March 7, 2001 (0A5399).

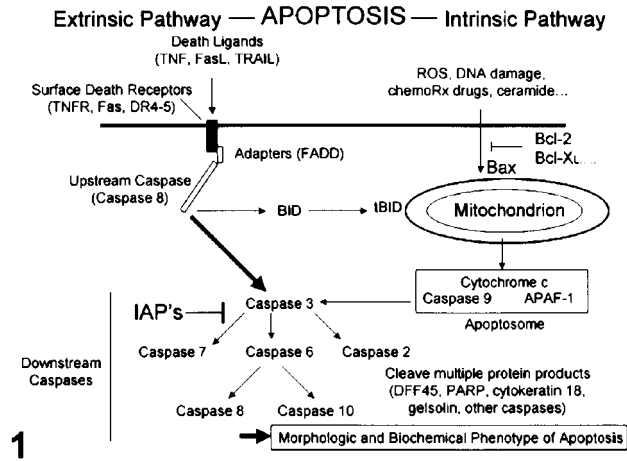


Figure 1 Diagrammatic summary of some of the biochemical steps in apoptotic pathways.

compared surface morphological (time-lapse phase-contrast), nuclear morphological (DAPI labeling), and ISNT (biotin-labeled) assays of apoptosis (Collins et al. 1997; Willingham 1999). Our current studies confirm the difficulties in the interpretation of the in situ end-labeling techniques (ISEL) such as ISNT (or TUNEL), and annexin V assays, but highlight the promising nature of the detection of caspase cleavage products for both cell culture and intact tissues.

Materials and Methods

Cells

KB is a continuous human carcinoma cell line related to HeLa cells. PC3 is a continuous human prostate carcinoma cell line. These cells were obtained from the American Type Culture Collection (Rockville, MD) and were grown in RPMI-1640 medium supplemented with 10% fetal calf serum and penicillin-streptomycin (Sigma; St Louis, MO) at 37°C in a 95% air/5% CO₂ atmosphere. Cells were subcultured using 2.5% trypsin with 1 mM EDTA.

Chemicals

Annexin V labeled covalently with fluorescein isothiocyanate (FITC) was obtained from Pharmingen (San Diego, CA). Alexa 568-annexin V was obtained from Boehringer-Mannheim Biochemicals (Indianapolis, IN). DAPI (4,6-diamidino-2-phenylindole), ricin toxin, and Dulbecco's PBS were obtained from Sigma. Mouse monoclonal anti-BUDr antibody (clone B44) was obtained from Becton-Dickinson (San Jose, CA). Mouse monoclonal anti-cytokeratin 18 was obtained from Chemicon (Temecula, CA) and a mouse monoclonal antibody reactive with the caspase-cleavage product of cytokeratin 18 (M30) (Leers et al. 1999) was obtained from Boehringer-Mannheim. All secondary and tertiary labeled anti-globulin antibodies and crystalline bovine serum albumin (BSA) were from Jackson ImmunoResearch (West Grove, PA). Bodipy-dUTP was obtained from Molecular

Probes (Eugene, OR) and Klenow fragment of *E. coli* DNA polymerase I was obtained from Sigma.

Experimental Design

Apoptosis in KB and PC3 cells was induced using ricin at 1 µg/ml as previously described (Collins et al. 1997). As shown in Figure 2, these conditions induce cell rounding in KB cells beginning within 4 hr, with all KB cells entering apoptosis in 24 hr. A subpopulation of PC3 cells entered apoptosis readily, but some PC3 cells were resistant to apoptotic entry up to the 24-hr time point (results not shown).

ISNT Labeling

ISNT was performed using a method similar to that previously presented (Collins et al. 1997). In one approach, dUTP incorporation into DNA strand breaks was assayed using Bodipy-labeled dUTP (Molecular Probes). In other experiments, we employed a modification of a BUDr labeling method (Szabo et al. 1987). Positive controls included the use of DNase treatment (1 U/µl in 1 mM Mg₂SO₄ and 1% BSA in Tris-buffered saline; 1 hr, 23°C). The ISNT reactions were stopped using a 5-min incubation in 0.5 M EDTA (pH 8.0).

Cells in 35-mm dishes were induced to enter apoptosis using ricin (from 4 to 24 hr, depending on the experiment) as described above, and floating cells were recovered from

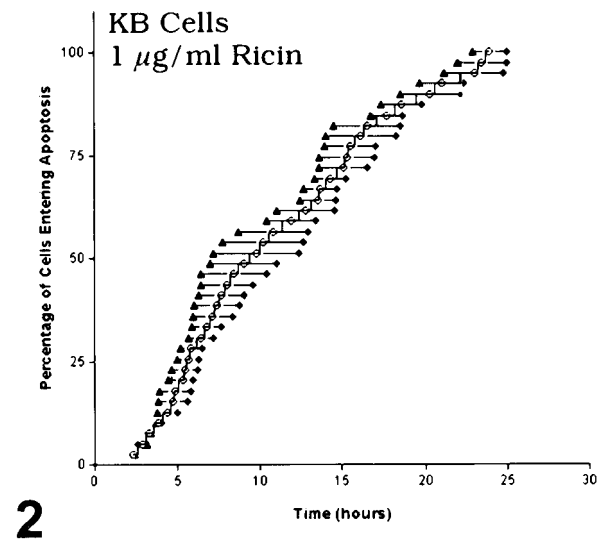


Figure 2 Detection of entry into apoptosis using video time-lapse microscopy. KB cells were induced to go into apoptosis by addition of ricin (1 µg/ml) to their medium at time 0. The flask of cells was placed on the stage of a warmed, inverted phase-contrast microscope for 24 hr and a record of cell morphology was made at a time-lapse ratio of 600:1. Entry into apoptosis was detected initially by cell rounding and blebbing. Each cell in the field was counted and the time of rounding and blebbing noted. The order of apoptotic entry is plotted on the ordinate vs the time of the initial cell blebbing on the abscissa. Two portions of the same video field were quantitated in this way and are shown as separate data points by either triangles or diamonds. The mean of the two is shown as circles. Note that 100% of the cells within the field entered apoptosis within the 24-hr time span.

the dishes, centrifuged, and resuspended in serum-free medium. The floating cells were reattached to 35-mm dishes that had been previously coated with poly-L-lysine (1 mg/ml in PBS for 5 min, washed in PBS) by centrifugation at 700 rpm ($200 \times g$) using a swinging bucket plate rotor (Sorvall RTH-750). Both attached and adherent cells were then fixed in 3.7% formaldehyde in PBS for 10 min at 23°C, followed by permeabilization with 0.2% Triton X-100 for 5 min.

The ISNT reaction mix (50 μ l) using Bodipy labeling was then added to PBS-washed attached and reattached cells, and spread over the dish by overlaying the cells with a coverslip and incubating for 1 hr at 37°C. The mixture consisted of water (37 μ l), $10 \times$ Klenow buffer (5 μ l), 10 mM dATP, dCTP, and dGTP mix (4.5 μ l), 1 mM Bodipy-dUTP (0.5 μ l), and 10 U of Klenow enzyme (2 μ l). After washing, the cells were postfixed in formaldehyde and mounted under a coverslip in glycerol.

For BUdR labeling, we modified the procedure of Szabo et al. (1987) as shown in Figure 3. The details of the fixation, permeabilization (0.2% Triton X-100), reaction mix, and antibody labeling are also shown in this figure. The affinity-purified secondary and tertiary antibodies were at 25 μ g/ml in PBS containing 1% BSA. The volume of the reaction mixture was 1 ml or greater, allowing incubation in dishes without the use of an overlying coverslip. A key difference in this protocol that is not present in the Bodipy labeling method is the use of an acid treatment step after the ISNT reaction to render the BUdR accessible to the mouse anti-BUdR antibody. For peroxidase labeling (as in Figure 6), the secondary anti-mouse IgG was conjugated to horseradish peroxidase, rather than rhodamine, and a tertiary anti-goat IgG labeled with peroxidase was also used. This peroxidase was detected using diaminobenzidine- H_2O_2 in PBS.

Annexin V Labeling

For analysis of fluorescent annexin V binding, cells in 35-mm dishes were removed from the 37°C incubations, cooled to 4°C, and washed in a binding buffer containing 2.5 mM $CaCl_2$, 140 mM NaCl, 20 mM Tris-HCl, pH 7.5. Labeled annexin V was added to cells at 1 μ g/ml in binding buffer and incubated at 4°C for 1 hr. For initial experiments, the cells were then washed free of unbound annexin V and fixed

in 3.7% formaldehyde at room temperature in PBS, then further incubated with formaldehyde in PBS together with 0.1 μ g/ml DAPI to label nuclear DNA at 4°C overnight. The attached cells were then washed in PBS and mounted under a drop of glycerol under a #1 circular 25-mm diameter coverslip in the dish. The dish was then viewed using a Zeiss Axioplan 2 upright fluorescence microscope equipped with a stage plate designed to hold 35-mm dishes.

Immunocytochemistry/Immunohistochemistry

PC3 cells grown in 35-mm culture dishes were fixed using 80% acetone in water for 10 min. The cells were then incubated in 1% bovine serum albumin-PBS saline (BSA-PBS) for 10 min, then mouse anti-cytokeratin 18 (10 μ g/ml; Chemicon #MAB3234) or mouse anti-caspase cleaved cytokeratin 18 (clone M30; Boehringer-Mannheim #2140322, 1:20 dilution) in BSA-PBS for 30 min at 23°C. This was followed by washing in PBS, then by serial incubations in affinity-purified goat anti-mouse IgG-rhodamine, followed by rabbit anti-goat IgG-rhodamine for signal amplification (25 μ g/ml; Jackson ImmunoResearch) in BSA-PBS. The dishes were then postfixed in 3.7% formaldehyde in PBS and viewed after mounting under a coverslip in glycerol. For induction of apoptosis, PC3 cells were incubated in 1 μ g/ml ricin for 24 hr. To select for apoptotic cells, floating cells were collected, washed in serum-free medium, then reattached by centrifugation onto poly-L-lysine coated dishes before fixation. These cells were also subsequently stained using DAPI to visualize nuclear morphology after the final formaldehyde fixation following antibody labeling.

For immunohistochemistry using MAb M30 on paraffin sections, sections were deparaffinized routinely, treated with Antigen Unmasking Solution (Vector Labs; Burlingame, CA) while heating in a microwave for 10 min, treated with 3% hydrogen peroxide in PBS, then incubated with mouse MAb M30 (1:20 dilution in BSA-PBS) for 30 min, followed by sequential incubations with affinity-purified goat anti-mouse IgG-horseradish peroxidase, followed by rabbit anti-goat IgG-peroxidase (25 μ g/ml; Jackson ImmunoResearch). The peroxidase was detected using diaminobenzidine-peroxide in PBS and counterstained with hematoxylin.

Microscopy

For time-lapse microscopy, cells in T-25 flasks were viewed under continuous incubation conditions using a Zeiss Axiomvert phase-contrast microscope equipped with a warm stage and an atmospheric controller as previously described (Collins et al. 1997). Video time-lapse recordings were made at a 600:1 time lapse (one frame every 10 sec) using a Panasonic time-lapse video cassette recorder. The resulting videotape record was examined using a Macintosh 8600 computer equipped with video frame grabber software. For quantitation of apoptosis, a single frame image was printed at time 0 and individual cells were numbered. Each cell was then followed during the 24-hr video recording, and the time of its entry into apoptotic blebbing was noted.

Fluorescent samples were viewed using a Zeiss Axioplan fluorescence microscope equipped with filters for UV excitation (DAPI), blue light excitation (FITC), and green light excitation (Alexa 568 or rhodamine). The images on individ-

BUdR-Hapten ISNT in Cultured Cells

(modified from Szabo, et al., Exp. Cell Res. 169: 158, 1987)

- 1) Fix (3.7% formaldehyde, PBS)
- 2) Permeabilize (Triton X-100)
- 3) {+/- DNAase control}
- 4) Reaction Mix (1 hr., 23°C)
- 5) Post-treatment: 2.5 M HCl,
0.25% Triton X-100 (20 min)
- 6) Mouse anti-BUdR (10 μ g/ml)
- 7) Goat anti-mouse IgG -Rhodamine
- 8) Rabbit anti-goat IgG-Rhodamine
(amplification step)

<p>Reaction Mix: BUdR triphosphate (300 μM) E. coli DNA polymerase I (50 units/ml) dATP, dGTP, dCTP (300 μM each) Tris-HCl (50 mM) MgSO₄ (10 mM) DTT (0.1 mM) pH 7.2 50% glycerol*</p>
--

3

*50% glycerol allows multiple re-use and freezing of the reaction mix

Figure 3 Modified BUdR-labeled ISNT protocol.

ual channels were captured using a SPOT cooled CCD digital camera, or a Dage 300 CCD camera. These images were either retained as grayscale images or recombined as color images with the three channels in overlay using Adobe Photoshop (4.0) software. All of the images shown in the figures represent digital images reproduced at >300 dpi.

Results

The model system for apoptosis employed in our studies involves the induction of cell death in KB cells, a human carcinoma cell line closely related to HeLa cells. We have also used these same assays with PC3 cells, a human prostate carcinoma cell line. Apoptosis was induced in these cells through the use of ricin, the toxic lectin of the castor bean plant. Ricin binds to cells, internalizes through surface clathrin-coated pits into endosomes, and eventually translocates through intracellular membranes into the cytosol, where it irreversibly inactivates ribosomes, inhibiting protein synthesis (reviewed in Tagge et al. 1997). Whether only through this action or through other effects, ricin induces apoptosis in a wide variety of cells. In our model system, the addition of 1 $\mu\text{g/ml}$ of ricin to culture medium results in the initiation of apoptotic surface blebbing in some KB cells within a few hours, and initiates apoptosis in all cells by 24 hr. An analysis of the beginning of apoptotic blebbing in two fields detected by time-lapse video phase-contrast microscopy in cultured KB cells is shown in Figure 2. This highly reproducible system allows careful comparison of the other detection methods for apoptosis at defined points in the process.

ISNT Labeling

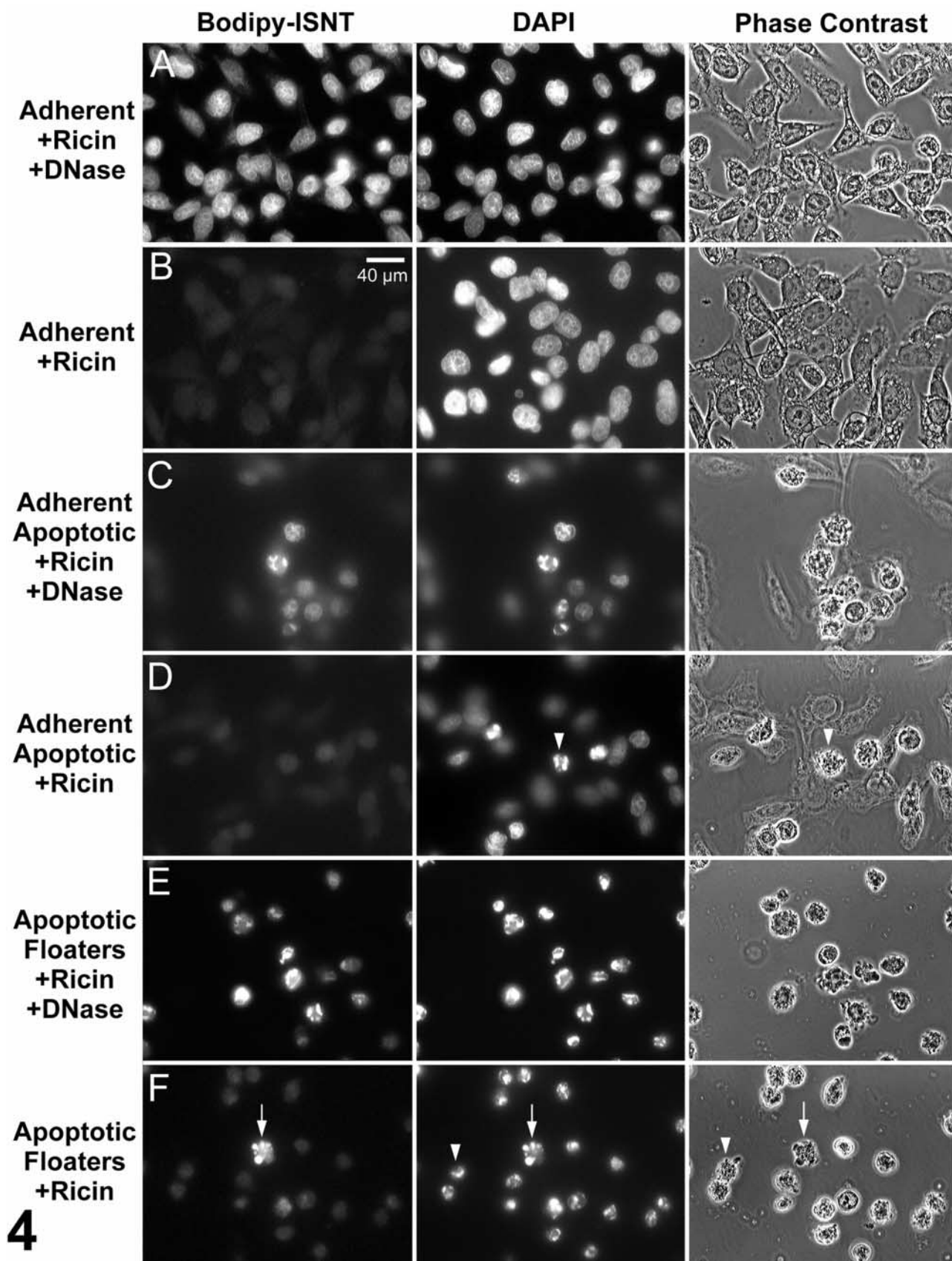
ISNT is one method of in situ end-labeling (ISEL) for detecting strand breaks in DNA that occur during apoptosis. Although different enzymes are used in the reaction mix, ISNT and TUNEL assays are closely related. We have chosen to use ISNT rather than TUNEL because, in our experience, ISNT has usually given a stronger signal in cultured cells. Figure 4 shows the use of an ISNT assay in the KB-ricin system in which the incorporated nucleotide is directly labeled using Bodipy-conjugated dUTP. Bodipy labeling has, in our experience, produced brighter fluorescence signals in comparison to some other fluorescent markers, such as FITC. The left panels in this figure dem-

onstrate ISNT labeling, the center panels demonstrate nuclear morphology using DAPI to label nuclear DNA, and the right panels show the phase-contrast appearance of the cells in each field. When cells undergo apoptosis in this system, cells that enter apoptosis often round up and can be washed from the culture dish. Analysis of these suspended cells provides a high frequency of apoptotic cells, while the cells attached to the plate are often not yet in apoptosis. Figure 4A shows attached cells that have been treated with DNase after fixation, rendering their nuclear DNA sufficiently fragmented to provide a positive control for the ISNT reaction. In Figure 4B, however, the otherwise untreated attached ricin-treated cells fail to show any ISNT signal.

In Figure 4C, some apoptotic cells appear rounded yet have failed to detach from the plate. Such cells show a strong ISNT signal when treated with DNase. However, in the absence of DNase treatment (Figure 4D) most of these cells fail to show an ISNT reaction. This indicates that the ISNT reaction can work in such cells but that most of these apoptotic cells are ISNT-negative at this point. To enrich for cells that have proceeded further into apoptosis, we isolated cells floating in the medium. Figure 4E shows that such cells, when reattached using poly-L-lysine-coated dishes, can be labeled with ISNT when they are treated with DNase after fixation. However, most of these cells are not labeled with ISNT in the absence of DNase treatment (arrowhead in Figure 4F). On the other hand, a few cells in the floating population show labeling with ISNT in the absence of DNase treatment (Figure 4F), and these cells have rounded morphology and segmented nuclear DNA (arrow in Figure 4F). These are the cells that would be labeled with methods such as TUNEL that detect DNA single strand breaks. It is evident from Figure 4F, however, that there are many other cells with the same morphological features (e.g., arrowheads) that fail to label with the ISNT method. Therefore, such methods appear to label only a minority of cells in a heterogeneous population at the early stages of induction of apoptosis, and confirm our prior findings that such labeling in most cells is a late event in the apoptotic process (Collins et al. 1997).

Although Bodipy labeling produces a strong signal in the ISNT reaction, the labeled substrate is rather expensive, comparable to the cost of biotin- and

Figure 4 ISNT of apoptotic KB cells using Bodipy labeling. KB cells were treated with ricin (1 $\mu\text{g/ml}$) for 6 hr. Then floating and adherent cells were separated and floaters were attached to new plates with poly-L-lysine, followed by fixation and permeabilization. ISNT was performed using Bodipy-labeled dUTP with (A,C,E) or without (B,D,F) treatment with DNase as a positive control for the ISNT labeling system. The dishes were post-stained using DAPI to visualize nuclear shape. Bodipy, DAPI, and phase-contrast images of the same fields are shown. As described in Results, adherent (A–D) and floating (E,F) cells showed that the majority of apoptotic cells (D,F, arrowhead) failed to show an ISNT signal at this time, although a few apoptotic floating cells were positive (F, arrow). Original magnification $\times 167$.



4

digoxigenin-labeled commercial substrates for ISNT and TUNEL reactions. This has often necessitated the use of the smallest possible reaction mix volumes, usually requiring the use of coverslips over cells and often resulting in damage to cells on the culture dish. We attempted to design a system that would be less expensive and allow the use of larger volumes of reaction mix. We employed the use of BUdR-triphosphate as previously described by Szabo et al. (1987). This allows a considerable decrease in cost and consequently allows the inexpensive preparation of larger volumes of reaction mix. A similar approach using terminal transferase with PAP labeling of Epon sections has been previously described (Aschoff et al. 1996). The final reaction conditions chosen are shown in Figure

3. This method utilized rhodamine fluorescence detection but could be readily adapted for other markers. The use of glycerol in the reaction mix also allows it to be frozen and re-used multiple times.

Figure 5 demonstrates the results in PC3 cells, both normal and apoptotic, using this BUdR-ISNT labeling system. Interestingly, when untreated cells were examined with this system, no signal was detected in normal nuclei, as expected (Figure 5A''). However, unexpectedly, a significant signal was detected in organelles with the morphological appearance of mitochondria. We had previously detected a similar pattern using a biotin-labeled ISNT system but had assumed that this background was due to endogenous biotin in mitochondria. However, the present system

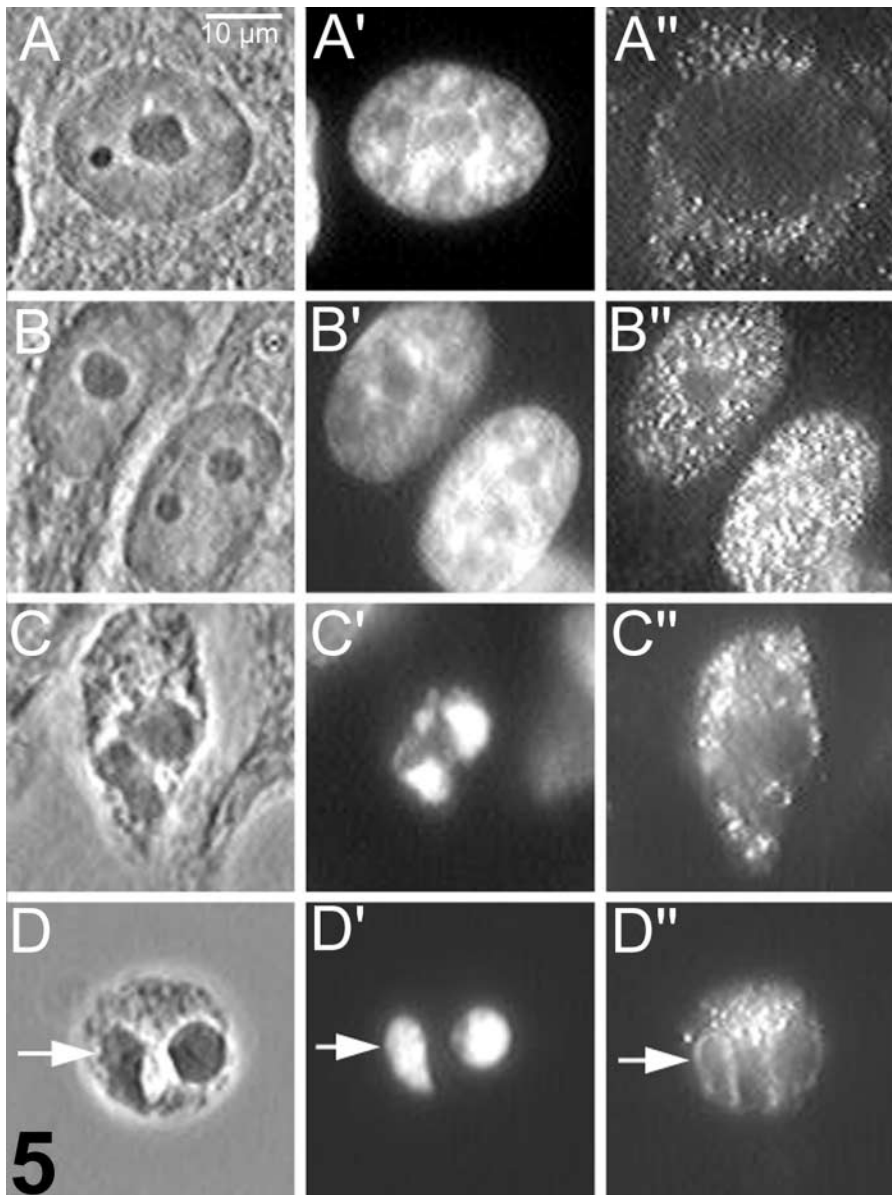


Figure 5 ISNT-BUdR labeling in normal and apoptotic cells. PC3 cells were exposed to ricin, fixed, permeabilized, and reacted with the BUdR-labeled ISNT procedure described in Figure 3. Cells were either treated (B) or untreated (A,C,D) with DNase as a positive control for the labeling system. The panels shown demonstrate phase-contrast (A–D), DAPI labeling (A'–D'), and BUdR-ISNT images (A''–D'') of the same cells. (A) A normal cell with no labeling in the nucleus but labeling present in structures with a shape and distribution consistent with mitochondria. (B) A cell after DNase treatment, showing a strong ISNT signal in the nucleus (B'), and loss of the "mitochondrial" signals. (C,D) Apoptotic cells, with labeling at the edge of condensed chromatin in D'. Original magnification $\times 830$.

does not use biotin, which suggests that this ISNT method may be labeling normal mitochondrial DNA. When these cells were treated with DNase after fixation (Figure 5B'), the nuclear DNA labeled strongly but the apparent mitochondrial signal disappeared, perhaps suggesting that the mitochondrial DNA was completely cleaved and not preserved. Apoptotic cells could be found that showed significant mitochondrial signal, but minimal nuclear signal (Figure 5C''), although some apoptotic cells were found that showed peripheral labeling of the nuclear segments (Figure 5D''). Similar to the Bodipy-labeled experiment in Figure 4, however, most apoptotic cells failed to label strongly with this ISNT method, in agreement with our previously published biotin-labeled results (Collins et al. 1997).

We also wished to examine the use of this ISNT method using peroxidase labeling. Figure 6 demonstrates an experiment in which cells were labeled with the reaction shown in Figure 3, but subsequently labeled with peroxidase instead of rhodamine. Fixed and permeabilized normal cells showed the same "mitochondrial" pattern using HRP labeling seen with rhodamine, and cells treated with DNase as a positive control showed loss of mitochondrial labeling and gain in nuclear labeling, similar to the results using rhodamine (Figure 5). These results suggest that the BUDR-ISNT method shown is an inexpensive and accurate ISNT method useful for various labeling techniques.

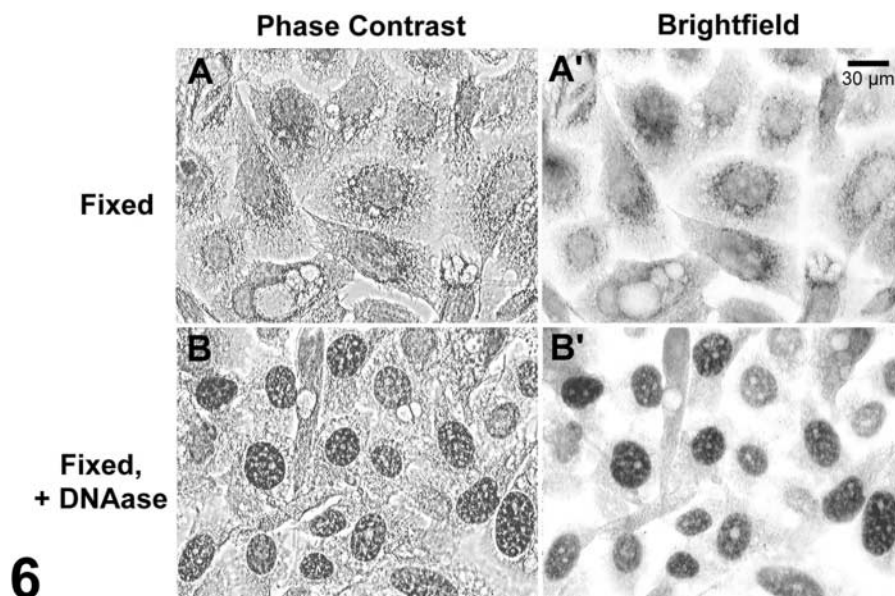
Annexin V Labeling

Annexin V is a protein that binds in a calcium-dependent manner to exposed phosphatidylserine (PS). When cells undergo apoptosis, PS normally sequestered on

the cytoplasmic face of the plasma membrane appears on the exterior of the cell where it can bind to labeled annexin V. Several labeled versions of annexin V are commercially available, and previous reports have described the use of this marker as an assay of apoptosis (Koopman et al. 1994; Bratton et al. 1997; Zhang et al. 1997; Gatti et al. 1998). One important issue in the use of annexin V labeling is whether the cells have proceeded through the entire apoptotic process and ultimately lysed, resulting in access to intracellular PS sites, an event that can also occur in necrotic cells. Another issue related to annexin V binding is whether all apoptotic cells externalize PS or whether only a subpopulation of apoptotic cells do so.

We examined annexin V binding during apoptosis with fluorescently-labeled derivatives using either FITC or Alexa 568 as marker in the KB-ricin model system. Figure 7 shows KB cells treated with ricin for 6 hr, then labeled with FITC-annexin V. Apoptotic cells were easily identified on the basis of their rounded, blebbing morphology and the segmentation of their nuclei detected using DAPI. Some of these cells subsequently incubated with annexin V at 4°C showed surface binding of FITC-labeled annexin V, but a significant number failed to show surface labeling (Figure 7A'). We quantitated this event at various times of ricin treatment, as shown in Figure 8. After a lag of 4 hr, cells began to show rounded morphology and altered nuclear shape, and a fraction of these same cells labeled with annexin V. Even at 22 hr after addition of ricin, however, when almost all cells have entered apoptosis, only about one third of the cells labeled with annexin V, even though each of these unlabeled cells showed the other surface and the nuclear morphological features of apoptosis.

Figure 6 ISNT-BUDr in normal PC3 cells using peroxidase labeling. Untreated PC3 cells were fixed and incubated as shown in Figure 5, except that the ISNT-BUDr reaction was detected with peroxidase-conjugated antibodies rather than rhodamine. The same apparent mitochondrial signal was detected in normal cells (A,A') as demonstrated by both phase-contrast (A,B) and brightfield images (A',B'). DNase treatment resulted in loss of the mitochondrial signal and gain of a nuclear signal (B,B'). Original magnification $\times 200$.



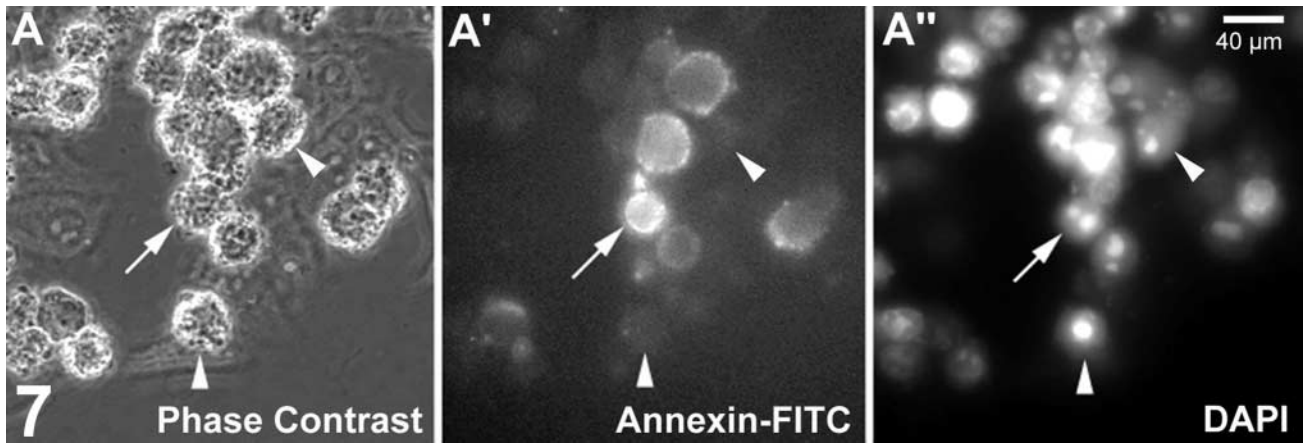
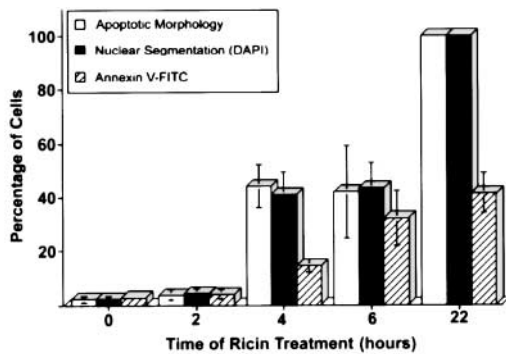


Figure 7 Detection of annexin V binding to the surface of apoptotic cells. KB cells were incubated with ricin ($1 \mu\text{g/ml}$) at 37C . At 6 hr, dishes of cells were removed from the incubator, cooled to 4C , washed, and incubated with FITC-labeled annexin V ($1 \mu\text{g/ml}$) for 1 hr. The cells were then washed in PBS and fixed in formaldehyde, together with DAPI, in PBS, followed by viewing using fluorescence microscopy. The same field of cells is shown in all of the panels. (A) Phase-contrast image; (A') the image on the fluorescein channel; (A'') the image on the DAPI channel. Note that some blebbing cells show strong annexin V labeling of their surfaces (arrow) as well as nuclear segmentation (A''). However, some cells (arrowheads) show blebbing (A) and nuclear segmentation (A'') but no annexin V labeling (A'). Original magnification $\times 175$.

One possible explanation for only a minority of apoptotic cells labeling with annexin V at these times was that our assay might have been performed at too early a time, and that cells might show progressive an-



8

Figure 8 Quantitation of morphological changes and annexin V binding in apoptotic cells. Cells in dishes from the experiment shown in Figure 7 were also examined individually for apoptotic morphology, nuclear segmentation, and annexin V binding at various times after ricin addition. At least 50 cells were examined and counted in each group. The percent of the total number of cells in the dish that showed these changes are plotted on the ordinate, with individual incubation times for each dish shown on the abscissa. Note that apoptotic morphological changes appear at 4 hr and, at that point, only about one third of those cells also show annexin V binding. This trend is also seen at a later time point (22 hr), at which most cells have begun apoptosis. Even then, only about one third of cells show annexin V binding. Note also, however, that the percentage of cells showing annexin V binding appears to increase between 4 and 6 hr, when the total percentage of apoptotic cells has increased only slightly. This suggests that apoptotic cells negative for annexin V binding might progress at a later time to show annexin V binding. Error bars represent 1 SD for each of the individual groups.

nexin V labeling at later times. To test this idea, we performed a double-label annexin V experiment in which KB cells were labeled with Alexa 568-conjugated annexin V at 6 hr after ricin addition, washed, and allowed to incubate at 37C for an additional 3 hr, and then labeled with FITC-conjugated annexin V. Figure 9 shows results from this experiment, in which some apoptotic cells failed to label at either 6 or 9 hr (Figure 9A, arrowheads), others labeled at both 6 and 9 hr (Figures 9A and 9B, arrow), and still others labeled only at 9 hr (Figure 9B, arrowhead). This might suggest that some apoptotic cells progress in their externalization of PS as they proceed through apoptosis.

If cells failed to label at 6 hr, it could also be due to the fact that they had not yet begun apoptosis. Therefore, we repeated this experiment using mechanical shaking selection to enrich for floating cells, in which almost all of the harvested cells had entered apoptosis on the basis of their surface morphology (results not shown). When we labeled these cells at 6 hr with Alexa-annexin V, washed, then labeled later at 9 hr with FITC-annexin V, we saw the results shown in Figure 10. Figures 10A''' and 10B''' are composite overlays of the images on individual channels shown in Figures 10A'-A''' and 10B'-B'''. Some cells showed apoptotic surface and nuclear morphology and did not label at either time with annexin V (results not shown). Other cells labeled at 9 hr but not at 6 hr (Figure 10B, arrow). In addition, some cells labeled at both 6 hr and 9 hr (Figure 10A). Interestingly, cells that had labeled at 6 hr showed internalization of the Alexa-labeled annexin V (Figure 10A''), indicating that apoptotic cells continue to endocytose material from their surfaces even though they have already begun to show other

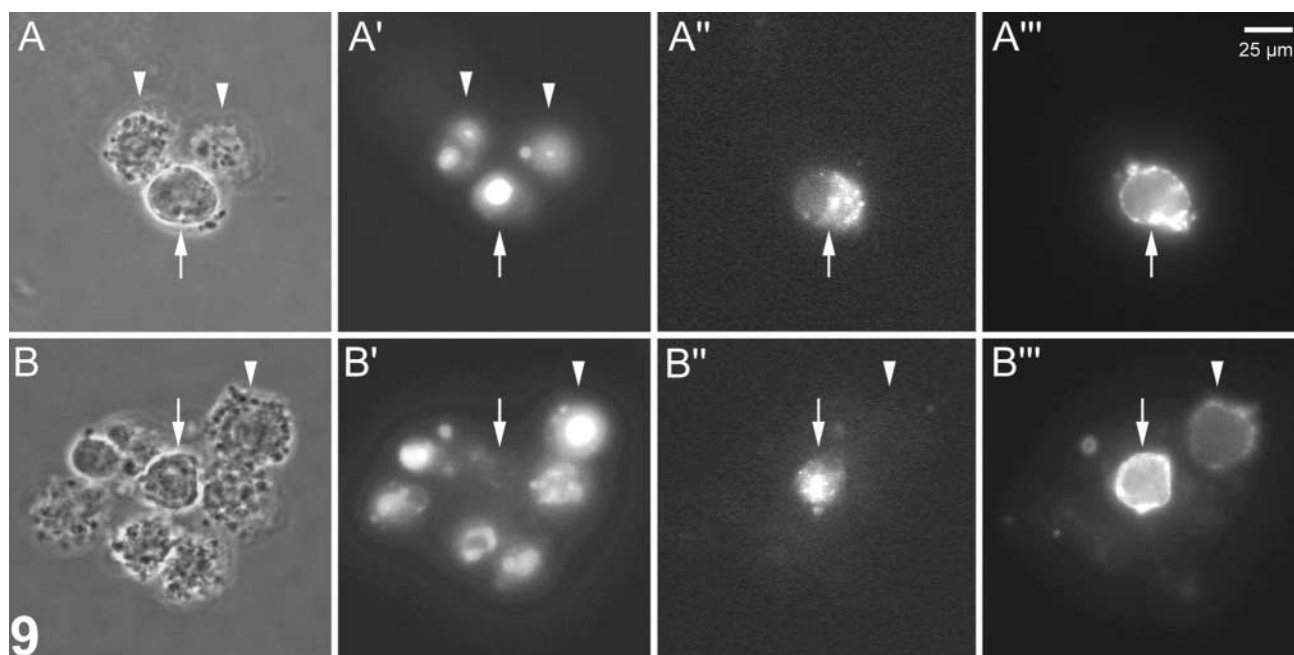


Figure 9 Double-label detection of annexin V binding at different times in the same cells. As described in Materials and Methods and in Results, cells were induced with ricin, then incubated with annexin V labeled with Alexa 568 at +6 hr, then incubated further at 37C until +9 hr, when they were incubated with FITC-labeled annexin V, followed by fixation. Phase-contrast images are shown in (A,B), DAPI channel images in (A',B'), Alexa channel images in (A''), and fluorescein channel images in (A'''). Note the central apoptotic cell in A (arrow) that shows altered nuclear morphology in A', internalized Alexa-annexin V in A'', and also surface FITC-annexin V in A'''. Other apoptotic cells (arrowheads) show altered nuclear morphology (A') but failed to label with annexin V at either 6 (A'') or 9 (A''') hr. On the other hand, note the cell in B (arrowhead) which shows nuclear segmentation in B', FITC-annexin V labeling in B''', but no Alexa-annexin V labeling in B'', suggesting that it did not label with annexin V at +6 hr. An apoptotic cell labeled at both times is shown by the arrow in B-B'''. Original magnification $\times 265$.

morphological changes typical of apoptosis. In other words, even though the cells have begun the process of dying, they still demonstrate at least one activity typical of living cells. Figure 10 also shows a cell (arrowhead) that demonstrates an interpretive problem with the use of annexin V, in that this cell has proceeded through the final lysis stage of apoptosis, allowing intense labeling of its internal PS directly. Such a result would also be seen with necrotic cells.

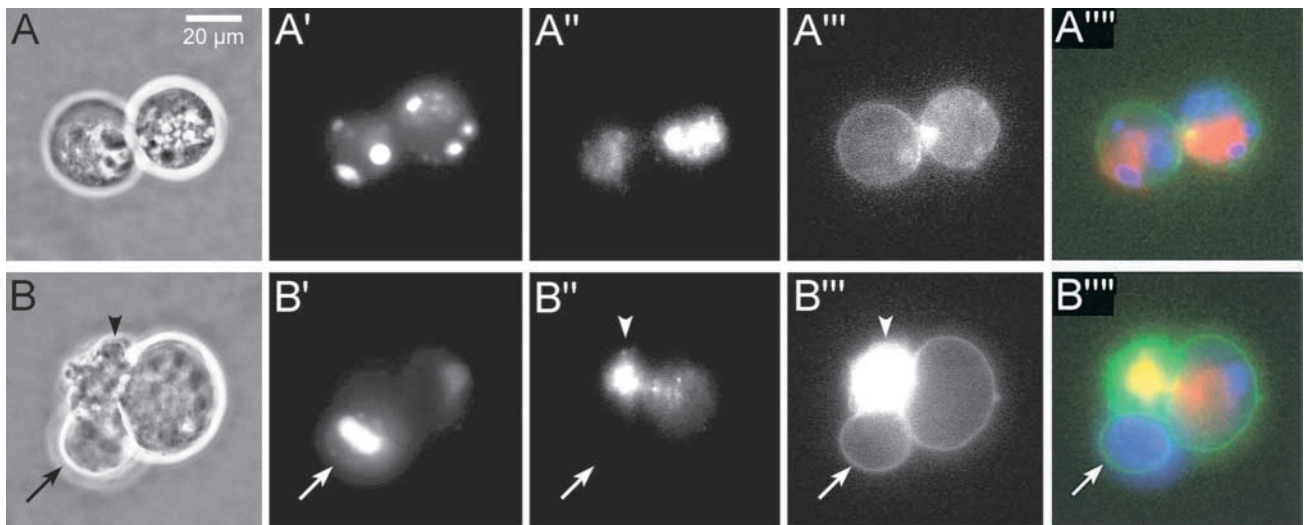
Detection of Caspase-generated Cleavage Products: Cytokeratin 18

Because caspase activity is likely to be the most specific indicator of the apoptotic process, assays of caspase activity through the detection of specific cleavage products in target proteins should represent a promising approach for measuring apoptosis. Such an approach could be applicable to fixed archival tissue blocks. We tested a recently commercially available antibody to the caspase-generated cleavage products of cytokeratin 18 (antibody M30) in PC3 cells, which can be shown to contain cytokeratin 18. This antibody (Leers et al. 1999) is similar in concept to other antibodies to cleaved keratins that have been previously reported (Caulin et al. 1997). Figure 11 shows

the presence of cytokeratin 18 in untreated PC3 cells (Figure 11A') using an antibody to intact cytokeratin. Figure 11 shows non-apoptotic cells from an experiment in which ricin was added to induce apoptosis in this same cell type. No reaction of MAb M30 was observed in such non-apoptotic cells. On the other hand, most cells showing apoptotic morphology (Figures 11C–11E) showed reaction with M30 in their cytoplasm, indicating the presence of caspase-cleavage products of cytokeratin 18. These results suggest that such an assay is potentially very useful for detecting apoptotic cells in cell culture. To confirm that this antibody could also be applied to fixed tissue sections, we examined M30 reactions detected by peroxidase labeling in an archival sample of human colon carcinoma. Figure 12 shows the positive reaction of this antibody selectively with cells with apoptotic morphology, suggesting that such an antibody is also useful in archival embedded tissues.

Discussion

Apoptosis is a central element in the pathogenesis of many disease processes and in the response to systemic therapies in neoplastic cells. Specific detection of apop-



10

Figure 10 Double-label detection of annexin V binding in disattached apoptotic cells. To confirm that the cells examined in Figure 9 were actually in apoptosis at +6 hr, the same experiment was repeated, but with selection (by shaking) of rounded disattached cells at the 6-hr time point. The cells were then further incubated until +9 hr and incubated with FITC-annexin V. In **A–A'''** note the rounded morphology by phase contrast in **A**, the nuclear segmentation on the DAPI channel in **A'**, the previously internalized Alexa-568-labeled annexin V in **A''**, and the surface labeling by FITC-annexin V at +9 hr in **A'''**. On the other hand, note the cell labeled with an arrow in **B**. This cell shows no Alexa 568 labeling (**B''**), but strong FITC-annexin V labeling (**B'''**), suggesting that this cell was apoptotic at +6 hr (based on selection by shaking) but that it had not yet externalized PS to its surface. The cell shown by the arrowhead has progressed further in apoptosis to the lysis stage and labels internally with FITC-annexin V (**B''''**). Also note that the intact cells in **A''** and **B''** show internalized Alexa-annexin V which was originally present on the cell surface at +6 hr. This demonstrates that, even though the cells had become apoptotic before +6 hr, they continued endocytosis at least until +9 hr. **A''''** and **B''''** are color overlays of the separate channels shown as grayscale images in **A'**, **B'**, **A''**, **B''**, and **A'''**, **B'''**. Original magnification $\times 367$.

tosis in tissue cells is therefore an important cytochemical technique for biomedical studies. The methods developed over the past decade for the detection of apoptosis have often been derived from empirical observations of the properties of dying cells. Recently, however, the molecular and biochemical mechanisms of apoptotic death have been further defined, leading to the prospect of assay methods based on highly specific chemical changes (Green 2000). Of the assays previously employed for apoptosis detection, those that are applicable to intact preserved tissues would have the broadest utility. One approach, the detection of DNA fragments through TUNEL or ISNT techniques, has been used extensively. Although useful, there are issues of specificity and interpretation of such techniques that have inspired a search for more highly specific assays.

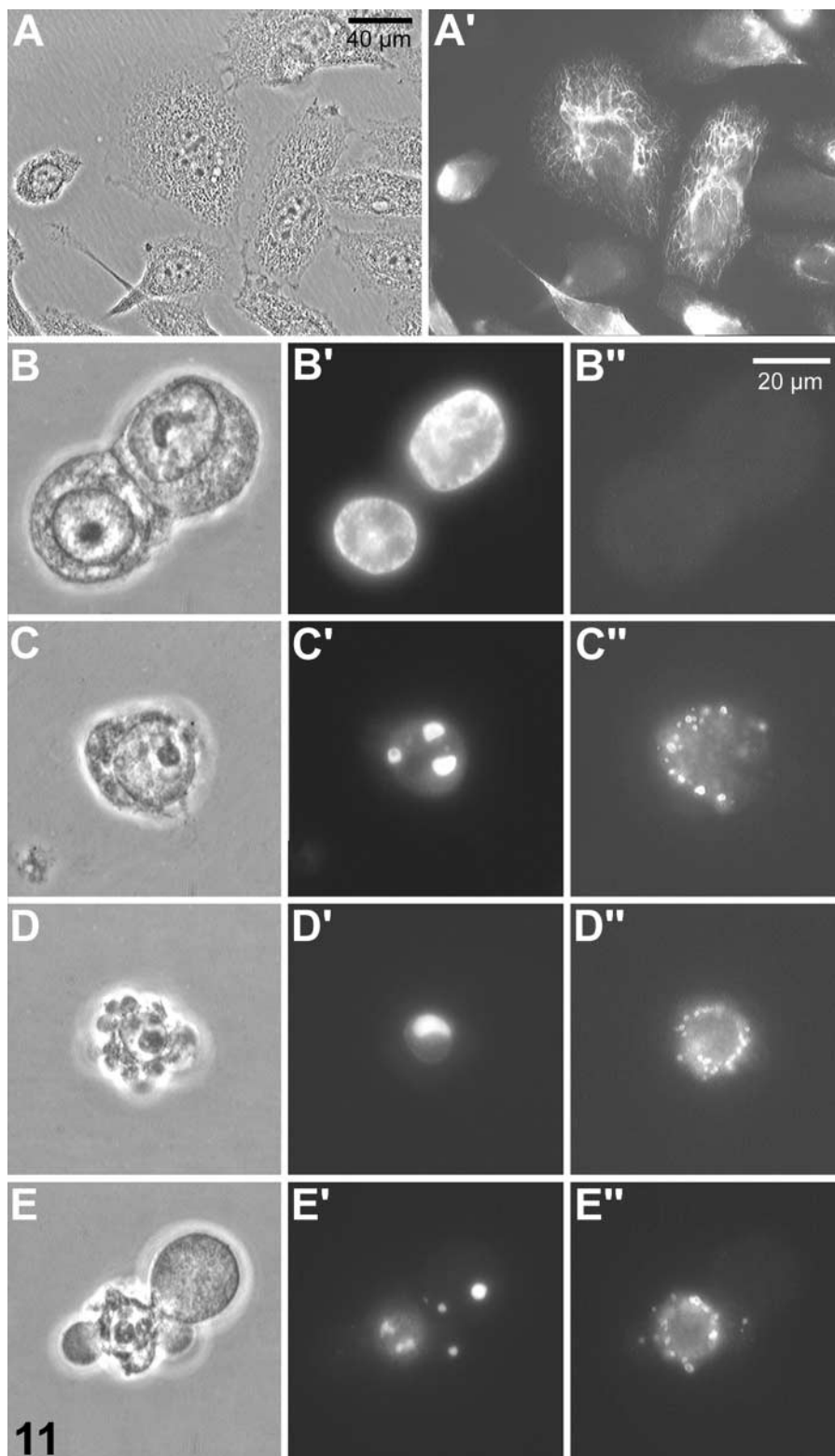
In this study, we have used a defined cell culture system, ricin-induced apoptosis in KB and PC3 cells, in which apoptosis can be induced in a highly synchronous and reproducible manner. The characteristics of this process are easily detectable at both the morphological and the biochemical level. We have applied some of the more promising recent cytochemical assays to this system. Because TUNEL and ISNT as-

says are perhaps the most commonly used cytochemical methods in this field, we have attempted to develop a less expensive alternative ISNT method to allow the use of larger reaction volumes for these assays. Through modification of an existing BUDR labeling method, we tested this method in the ricin-induced apoptosis system and found results similar to those previously reported (Collins et al. 1997), in which the ISNT reactions were seen as a late event in the apoptotic process in a minority of cells.

We also examined another commonly used cytochemical assay of apoptosis, the labeling of externalized PS by annexin V. Although this assay detects apoptosis at an earlier stage than ISNT, only a minority of apoptotic cells actually labeled with annexin V before the final lysis of cells at the end of the apoptotic process. This is in agreement with other studies published previously using a different apoptosis system (Gatti et al. 1998). The annexin V experiments did demonstrate, however, that cells appear to progress in their externalization of PS with time, and that cells already involved in the apoptotic process still demonstrate endocytic activity for many hours.

Finally, we examined one newly available antibody that detects the specific cleavage fragments of a cyto-

Figure 11 Detection of caspase-cleaved cytokeratin 18 in cultured cells. PC3 cells were initially demonstrated to contain intact cytokeratin 18 using an antibody reactive with the intact protein (A') using immunofluorescence. PC3 cells were then treated with ricin and examined using an antibody that reacts selectively with caspase-cleaved cytokeratin 18 (M30). Non-apoptotic cells in this culture failed to react with this antibody (B'') but apoptotic cells showed a bright cytoplasmic speckled pattern (C''-E''). [A-E, phase-contrast; A', anti-cytokeratin 18 (intact); B-E', DAPI; B''-E'', anti-cleaved cytokeratin 18 (antibody M30)]. Original magnifications: A $\times 250$; B-E $\times 600$.



plasmic target of caspases, cytokeratin 18 (Leers et al. 1999). Not only did this antibody detect apoptotic cells with high specificity in cell culture but it also showed reaction in archival tissue sections. Cytokera-

tin 18 is expressed only in certain cell types, however, and this antibody is not broadly applicable to all cell types. The use of antibodies specific for more generally distributed cleaved substrates of caspases, such as

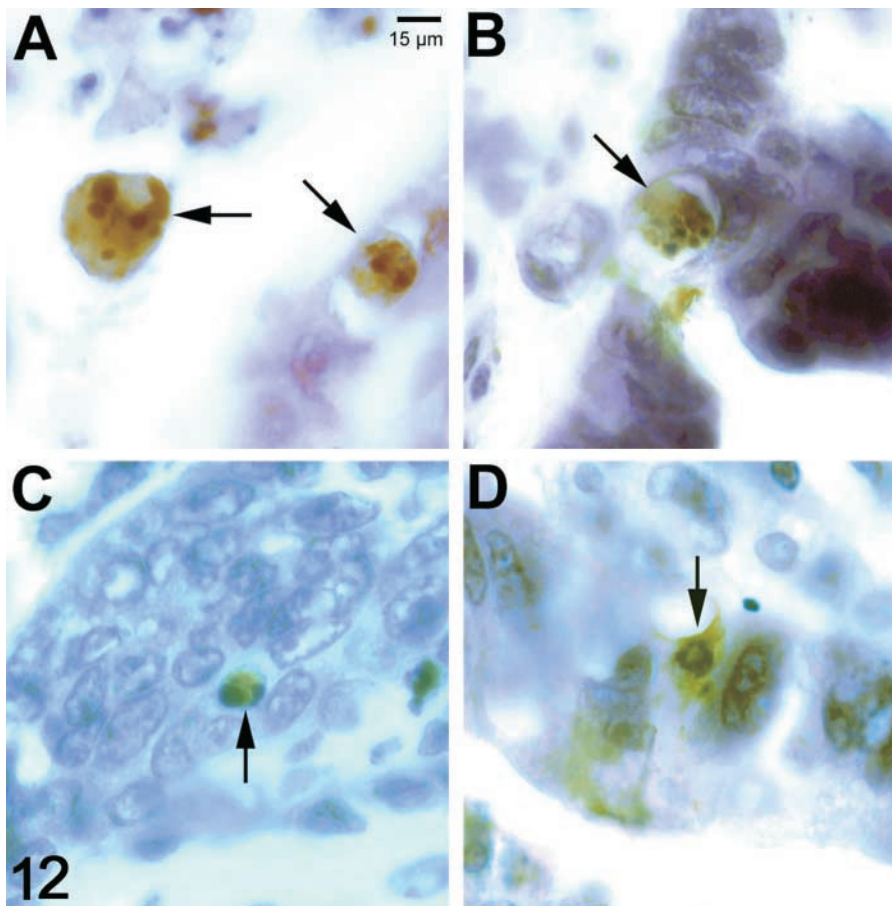


Figure 12 (A–D) Detection of caspase-cleaved cytokeratin 18 in paraffin sections. Sections of formalin-fixed, paraffin-embedded human colon adenocarcinoma were reacted with anti-cleaved cytokeratin 18 (M30) and labeled using peroxidase. These images show examples (arrows) of cells with apoptotic morphology that label strongly using this antibody. Original magnification $\times 320$.

the cleaved form of caspase 3, would have more general applicability.

Acknowledgments

We wish to thank Drs Timothy Kute and Arthur Frankel for helpful discussions. These results include data generated while JMW was the recipient of a summer student scholar research award from the South Carolina Governor's School.

Literature Cited

- Allen RT, Hunter WJ, Agrawal DK (1997) Morphological and biochemical characterization and analysis of apoptosis. *J Pharmacol Toxicol Methods* 37:215–228
- Aschoff A, Jantz M, Jirikowski GF (1996) In-situ end labeling with bromodeoxyuridine—an advanced technique for the visualization of apoptotic cells in histologic specimens. *Hormone Metab Res* 28:311–314
- Bratton DL, Fadok VA, Richter DA, Kailey JM, Guthrie LA, Henson PM (1997) Appearance of phosphatidylserine on apoptotic cells requires calcium-mediated nonspecific flip-flop and is enhanced by loss of the aminophospholipid translocase. *J Biol Chem* 272:26159–26165
- Caulin C, Salveson GS, Oshima RG (1997) Caspase cleavage of keratin 18 and reorganization of intermediate filaments during epithelial apoptosis. *J Cell Biol* 138:1379–1394
- Collins JA, Schandl CA, Young KK, Vesely J, Willingham MC (1997) Major DNA fragmentation is a late event in apoptosis. *J Histochem Cytochem* 45:923–934
- Gatti R, Belletti S, Orlandini G, Bussolati O, Dall'asta V, Gazzola GC (1998) Comparison of Annexin V and calcein-AM as early vital markers of apoptosis in adherent cells by confocal laser microscopy. *J Histochem Cytochem* 46:895–900
- Green DR (2000) Apoptotic pathways: paper wraps stone blunts scissors. *Cell* 102:1–4
- Koopman G, Reutelingsperger CP, Kuijten GA, Keehnen RM, Pals ST, van Oers NH (1994) Annexin V for flow cytometric detection of phosphatidylserine expression on B cells undergoing apoptosis. *Blood* 84:1415–1420
- Leers MP, Kolgen W, Bjorklund V, Bergman T, Tribbick G, Persson B, Bjorklund P, Ramaekers FC, Bjorklund B, Nap M, Jornvall H, Schutte B (1999) Immunocytochemical detection and mapping of a cytokeratin 18 neo-epitope exposed during early apoptosis. *J Pathol* 187:567–572
- Szabo G Jr, Damjanovich S, Sumegi J, Klein G (1987) Overall changes in chromatin sensitivity to DNase I during differentiation. *Exp Cell Res* 169:158–168
- Tagge E, Harris B, Burbage C, Hall P, Vesely J, Willingham M, Frankel A (1997) Synthesis of green fluorescent protein-ricin and monitoring of its intracellular trafficking. *Bioconjugate Chem* 8:743–750
- Willingham MC (1999) Cytochemical methods for the detection of apoptosis. *J Histochem Cytochem* 47:1101–1109
- Wyllie AH (1992) Apoptosis and the regulation of cell numbers in normal and neoplastic tissues: an overview. *Cancer Metastasis Rev* 11:95–103
- Zhang G, Gurtu V, Kain SR, Yan G (1997) Early detection of apoptosis using a fluorescent conjugate of Annexin V. *Biotechniques* 23:525–531